Neutron cryo-crystallography captures the protonation state of ferryl heme in a peroxidase

Cecilia M. Casadei[1,2], Andrea Gumiero[3], Clive L. Metcalfe[3], Emma J. Murphy[3], Jaswir Basran[1], Maria Grazia Concilio[4], Susana C. M. Teixeira[2,5], Tobias E. Schrader[6], Alistair J. Fielding[4], Andreas Ostermann[7], Matthew P. Blakeley[2], Emma L. Raven[3,*], Peter C. E. Moody[1,*]

1. Department of Biochemistry and Henry Wellcome Laboratories for Structural Biology, University of Leicester, Lancaster Road, Leicester LE1 9HN, UK.

2. Institut Laue-Langevin, 71 Avenue des Martyrs, 38000, Grenoble, France.

3. Department of Chemistry, University of Leicester, University Road, Leicester LE1 7RH, UK.

4. The Photon Science Institute, The University of Manchester, Manchester M13 9PL, UK.

5. EPSAM, Keele University, Keele, Staffordshire ST5 5BG, UK.

6. Jülich Centre for Neutron Science (JCNS), Forschungszentrum Jülich GmbH, Outstation at MLZ, Lichtenbergstraße 1, 85747 Garching, Germany.

7. Heinz Maier-Leibnitz Zentrum (MLZ), Technische Universität München, Lichtenbergstraße 1, D-85748 Garching, Germany.

*Corresponding author. E-mail: emma.raven@le.ac.uk (E.L.R.); peter.moody@le.ac.uk (P.C.E.M.)

Abstract

Heme enzymes activate oxygen through formation of transient iron-oxo (ferryl) intermediates of the heme iron. A long-standing question has been the nature of the iron-oxygen bond and, in particular, the protonation state. We present neutron structures of the ferric derivative of cytochrome c peroxidase and its ferryl intermediate; these allow direct visualization of protonation states. We demonstrate that the ferryl heme is an Fe(IV)=O species and is not protonated. Comparison of the structures shows that the distal histidine becomes protonated on formation of the ferryl intermediate, which has implications for the understanding of O–O bond cleavage in heme enzymes. The structures highlight the advantages of neutron cryo-crystallography in probing reaction mechanisms and visualizing protonation states in enzyme intermediates.

Aerobic organisms have evolved to use the intrinsic oxidizing power of oxygen from the atmosphere. This activation of oxygen is achieved by a catalytic metal center (usually iron or copper) buried within a protein. In the case of iron, high-valent iron-oxo (also known as ferryl) intermediates play a role in a large number of different, and sometimes difficult, biological oxidations catalyzed by various heme and non-heme iron-containing enzymes.

For the heme iron enzymes, the mechanism of oxidation involves initial formation of the iconic compound I intermediate (1, 2). Compound I contains an oxidized ferryl heme, plus either a porphyrin π-cation radical or a protein radical; reduction of compound I by one electron yields the closely related compound II intermediate, which contains only the ferryl heme. These compound I and II intermediates are a defining feature across the heme enzyme family and appear in a diverse group of catalytic heme enzymes that include all the cytochrome P450s, the nitric oxide synthases, and the terminal oxidases, plus the heme dioxygenases and heme peroxidases. Indeed, they are such crucial intermediates in so many processes—including many involved in drug metabolism and other important oxidations—that their structure and reactivity has become a key question for both heme (3–7) and non heme iron enzymes where similarly transient iron-oxo species are also employed (8, 9).

A long-standing and highly contentious question has been to clarify the bond order and protonation state of the ferryl heme. The question has focused on whether the ferryl is formulated as an Fe(IV)=O [iron(IV)-oxo] or Fe(IV)-OH [iron(IV)-hydroxide] species, but there are a number of reasons why previous methodologies—none of which can measure the protonation state directly—have failed to fully resolve the issue. To begin with, even capturing these transient intermediates in some enzymes [especially in the P450s (10, 11)] has proved very difficult. Early approaches to the problem used both extended x-ray absorption fine structure and resonance Raman methods [reviewed in (12)] to examine the iron-oxygen bond as an indirect reporter on the protonation state. These studies indicate a short Fe-O bond length, but the data were not totally consistent, and the photolability of compound I during laser excitation is well documented (13) so that interpretation of stretching frequencies from Raman work has not been unambiguous either. More recently, x-ray crystallographic methods have been employed. These methods showed longer iron-oxygen bond lengths, but the x-ray structures of compounds I and II were subsequently shown to have been affected by photoreduction of the iron and are now considered to be unreliable. The more recent use of multiple crystals in x-ray analyses minimizes photoreduction but cannot entirely eliminate the

problem. Moreover, hydrogen atoms are difficult to locate in electron density maps due to their weak scattering. Even if very high-resolution data (i.e., better than 1.2 Å) are available, hydrogen atoms can remain obscured due to their mobility. There is also the substantive question of whether such small changes in Fe-O bond length (<0.2 Å) between Fe(IV)=O and Fe(IV)-OH species, even if measured at high resolution and without photoreduction, are determined accurately enough in x-ray experiments to report reliably on the protonation state.

For these reasons, we have adopted a different approach. Neutron diffraction offers a more reliable solution to the problem, because hydrogen and, particularly, its isotope deuterium (D) are visible at much lower resolutions than required with x-rays (14, 15). The approach does present a number of challenges, particularly the need to cool the large crystals required for neutron crystallography down to the cryogenic temperatures required for the study of enzyme intermediates (16). But the fact that neutrons are non-ionizing and are scattered by the atomic nuclei (rather than by the electrons, as in x-ray crystallography) means that photoreduction, which has been the source of most of the confusion in previous x-ray work, does not occur at all. In the case of redox enzymes, the elimination of photoreduction is a considerable advantage if the other experimental challenges can be overcome.

In this work, we have used neutron crystallography to determine the structure of ferric cytochrome c peroxidase (CcP) and its transient ferryl intermediate. The structures allow us to visualize the positions of hydrogen and deuterium atoms in the enzyme, as well as to unambiguously identify the protonation state of the ferryl heme.

Cytochrome c peroxidase catalyzes the H2O2-dependent oxidation of cytochrome c. Compound I of CcP, formed rapidly from the reaction of ferric enzyme with peroxide, contains a ferryl heme plus a stable protein radical on Trp191 (17). It was the first peroxidase to be crystallized (18) and over many years has served as a model enzyme for the understanding of oxygen activation across the family of catalytic heme enzymes. We first solved the neutron structure of ferric CcP to 2.4 Å at room temperature. The structure was determined using x-ray and neutron diffraction data obtained from a D2O-exchanged crystal (see supplementary materials and methods; data and refinement statistics are shown in table S1).

Figure 1 shows nuclear scattering and electron density of ferric CcP in the region of the heme and summarizes the positions of all the hydrogen and deuterium atoms. On the distal side of the heme (Fig. 1, A and C), His52 is neutral as Nδ is deuterated but Nε is not. The Nε of Trp51 is deuterated; Arg48 is fully deuterated and positively charged. The neutron structure unambiguously identifies W1 as a heavy water molecule (D2O), rather than an OD– ion, at a distance of 2.7 Å from the iron. We assign the heme as five-coordinate. On the proximal side (Fig. 1, B and D), Nε of His175 is not deuterated and is 2.0 Å from the iron. The Nδ of His175 is deuterated and within hydrogen bond distance of the unprotonated Oδ2 of Asp235; likewise, Oδ1 of Asp235 is unprotonated and within hydrogen bond distance of the deuterated Nε of Trp191. Both heme propionates are unprotonated.

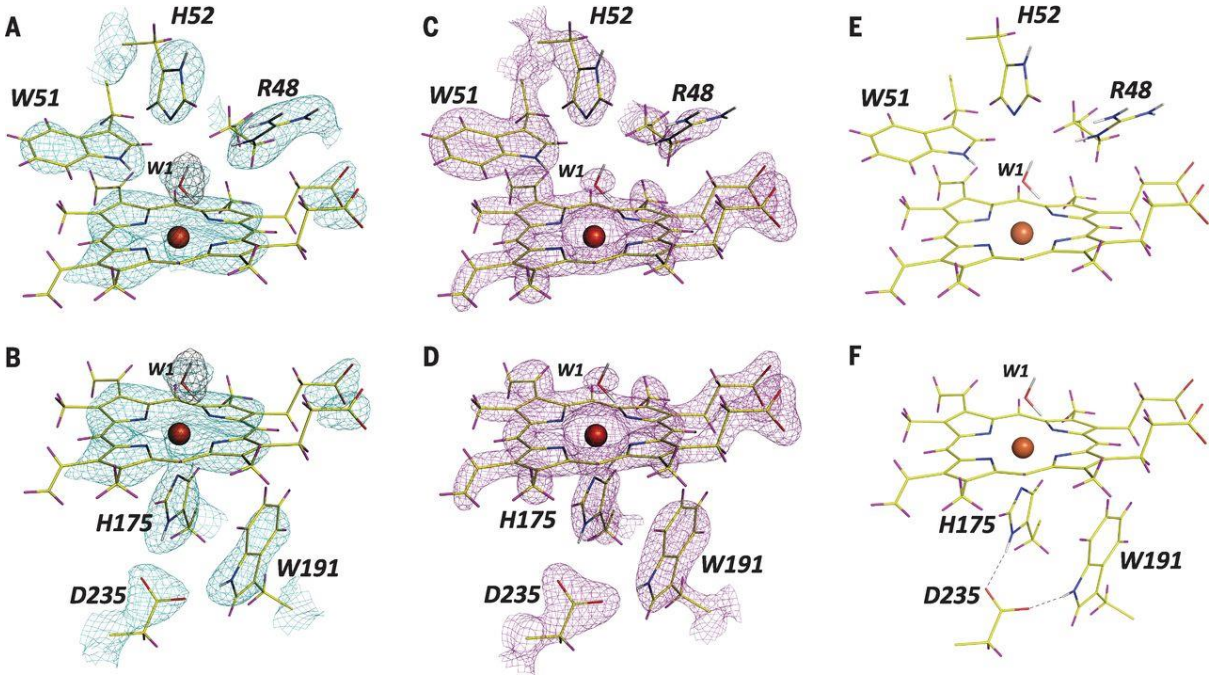

Fig. 1

The structure of ferric CcP in the region of the heme.

In the neutron experiment, neutrons are diffracted by the atomic nuclei (in contrast to x-rays, which are scattered by electrons). Hydrogen atoms (shown in magenta) have a negative coherent neutron scattering length (–3.74 fm), whereas deuterium atoms (shown in white) have a positive coherent scattering length (6.77 fm). Exchangeable hydrogen atoms, therefore, show up with density similar to carbon (6.65 fm) and oxygen (5.85 fm), whereas nitrogen has a greater scattering length (9.37 fm). The scatter from a methylene (CH2) group sums to nearly zero, so that at moderate resolution (~2 to 2.5 Å) cancellation of nuclear scattering density is observed, and the joint refinement allows

use of the x-ray terms to place the nonhydrogen atoms in these regions. Nuclear scattering density [σA-weighted 2Fo-Fc contoured at 2.6 root mean square (RMS)] in the (A) distal and (B) proximal heme pocket is shown in cyan. Electron density (σA-weighted 2Fo-Fc contoured at 2.4 RMS) in the (C) distal and (D) proximal pocket is shown in magenta. The black contour (σA-weighted neutron Fo-Fc contoured at 5.0σ) shows the difference density calculated by omitting the bound water (W1). Protonation states are depicted for (E) distal and (F) proximal active site residues. The distal pocket shows an ordered water molecule (W1) 2.7 Å away from the five-coordinate heme iron. W1 donates a hydrogen bond to the π orbitals of the porphyrin ring and may be a potential hydrogen bond acceptor to the deuterated Nε of Trp51. W1 may also interact with a poorly ordered water (not shown) that displaces the guanidinium of Arg48, which is seen in the "out" position (19). Color scheme: hydrogen atoms, magenta; deuterium, white; oxygen, red; nitrogen, blue; carbon, yellow; iron, orange sphere. Hydrogen bonds are shown as dashed lines. H, His; R, Arg; D, Asp; W (except W1), Trp.

Crystals of D2O-exchanged CcP (see supplementary materials and methods) were reacted with hydrogen peroxide as previously reported (19). Formation of compound I in CcP crystals is established [e.g., (20, 21)] but was verified in several ways. Single-crystal microspectrophotometry at 100 K on similar (smaller) crystals showed the characteristic absorption peaks in the visible region (530, 560, and 632 nm) (fig. S1A), in agreement with the literature (22). Spectra of these crystals were unchanged on storage over 20 days (fig. S1B). Single-crystal electron paramagnetic resonance (EPR) on similar crystals prepared and reacted in the same way (see supplementary materials and methods) also showed the appearance of the characteristic g = 2 signal from the Trp191 radical (17) (fig. S2); in solution, compound I of CcP is stable for hours at room temperature (23) and indefinitely at 77 K (figs. S3 and S4).

We then used x-ray and neutron diffraction data to determine the 2.5 Å resolution neutron structure of compound I of CcP at 100 K (see supplementary materials and methods). Figure 2 shows nuclear scattering and electron density in the region of the heme and summarizes the positions of all the hydrogen and deuterium atoms. Data and refinement statistics are shown in table S2. Nuclear scattering and electron density maps for individual active site residues are shown in fig. S5. In comparison to the ferric enzyme, most of the protonation states are retained in the compound I structure, with the exception of His52, which is now deuterated at both Nδ and Nε (fig. S5D). We observe that the Nε of the Trp191 radical is deuterated, which identifies the radical species as a

(protonated) π-cation radical (24). Compared to the ferric enzyme, Arg48 has moved into the heme pocket.

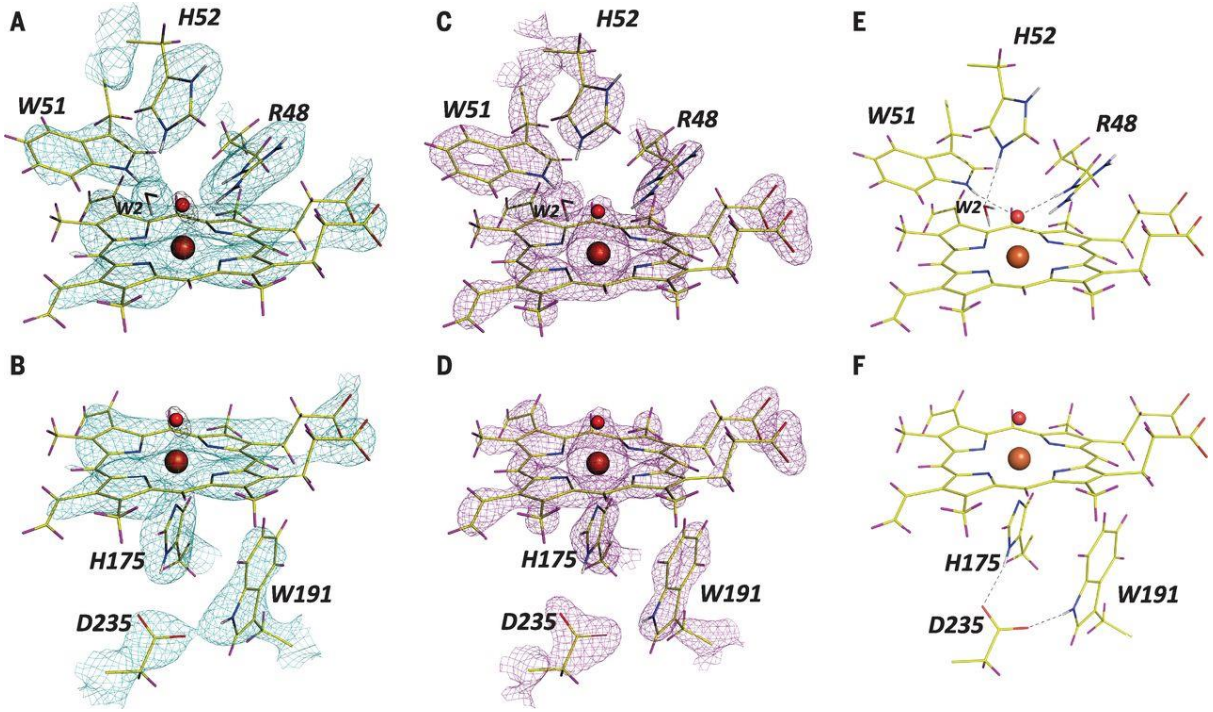

Fig. 2

The structure of compound I of CcP in the region of the heme.

Nuclear scattering density (σA-weighted 2Fo-Fc contoured at 2.2 RMS) in the (A) distal and (B) proximal heme pocket is shown in cyan. Electron density (σA-weighted 2Fo-Fc contoured at 2.6 RMS) in the (C) distal and (D) proximal heme pocket is shown in magenta. The black contour (σA-weighted neutron Fo-Fc contoured at 3.5σ) shows the difference density calculated by omitting the ferryl oxygen. Protonation states are depicted for (E) distal and (F) proximal active site residues. In the distal pocket, the ferryl oxygen acts as an acceptor for hydrogen bonds from the deuterated Nε of Arg48 and the deuterated Nε of Trp51. His52 is deuterated at both Nδ and Nε, the latter acting as a hydrogen bond donor to a bound water molecule (W2). W2 donates a hydrogen bond to the π orbitals of the porphyrin ring. Color scheme is as in Fig. 1, with the iron and ferryl oxygen depicted as orange and red spheres.

Analysis of the nuclear scattering density maps indicates that the ferryl oxygen is not deuterated in the structure. This is confirmed by examination of the hydrogen bond structure: The ferryl oxygen acts as a hydrogen bond acceptor to the Nε of Trp51 and to the Nε of Arg48, both of which are

accordingly deuterated. We interpret this geometry as consistent with an unprotonated Fe(IV)=O species. An Fo–Fc neutron map calculated in the absence of the ferryl oxygen shows a peak (3.8σ) in nuclear scattering density at 1.6 Å from the iron atom (Fig. 2, A and B), which is consistent with the most recent x-ray data [reported as 1.63 Å (19) and 1.73 Å (25)]. However, bond lengths cannot be determined precisely at this resolution and, as we note above, report only indirectly on the protonation state. The unambiguous observation from the neutron structure is that the oxygen is not protonated, which establishes that the ferryl intermediate is an Fe(IV)=O species at this pH. The neutron data show that there is no hydrogen bond from the distal histidine to the ferryl heme, as has been suggested previously (26) in horseradish peroxidase to account for pH-dependent spectroscopic behavior of the ferryl intermediate.

Mechanisms for O–O bond cleavage in peroxidases are invariably drawn (1, 27) showing the distal histidine (His52 in the case of CcP) as neutral in both ferric and compound I species, which assumes that both protons of H_2O_2 are used in the formation of a water molecule. Our data are not consistent with this long-standing description. His52 is indeed neutral in the ferric state (Fig. 1 and fig. S5E) but is deuterated on Nε and Nδ in compound I (Fig. 2 and fig. S5D). We take this to mean that the widely assumed role of the distal histidine in compound I formation—acting first as a base catalyst (to deprotonate peroxide) and then as an acid catalyst (to protonate the peroxide oxygen and release water)—needs to be reassessed.

Possible alternative mechanisms showing movement of protons during O–O bond cleavage are shown in Fig. 3. Ferric CcP is unprotonated on the Nε of His52, and the Nε lone-pair geometry does not interact ideally with any neighboring proton donors. This lack of ideal hydrogen bonding structure in the ferric form may favor formation of the peroxide complex and the deprotonated compound 0 (28), as structures of the closely related compound III (oxy) complexes all suggest that more favorable hydrogen bonding interactions with the bound peroxide are likely (fig. S6). Our data suggest that His52 retains a proton upon formation of compound I. In terms of proton count, this presumably means that delivery of an additional proton to compound 0 is needed for compound I formation if water is released as product (Fig. 3A), aligning the mechanism more closely with the related P450s in which delivery of a single proton to compound 0 is also widely assumed (2, 29). Arg48, which is protonated (Figs. 1 and 2), could act as the source of the additional proton required for release of water in both formation and reduction of compound I, as it is thought to play a role in proton-relay networks (30). Hydroxide (instead of water, Fig. 3A) formation is also possible; if this is

the case, a role for Arg48 in charge stabilization of OH– is easily envisaged and would be consistent with early predictions (31). Because the proton on His52 must be removed before a second turnover of the enzyme can occur, the acid-catalysis role of His52 must occur after compound I formation and not [as is often assumed (1)] before (Fig. 3A). An alternative and intriguing possibility (Fig. 3B), which could apply generally to any heme protein with a distal histidine in the heme pocket, is that O–O bond cleavage initially forms a transient Fe(IV)-OH species [as in the P450s (32)], but the presence of the distal histidine provides an escape route for the proton, thus disfavoring formation of Fe(IV)-OH. Proton transfer in this direction, to form Fe(IV)=O, would be consistent with published pKas (Ka, acid dissociation constant) for the distal histidine across the peroxidase family [estimated pKa ≈ 4 to 5 (1, 33)] if the pKa of the ferryl heme, which is not known reliably for a heme peroxidase, was lower than that.

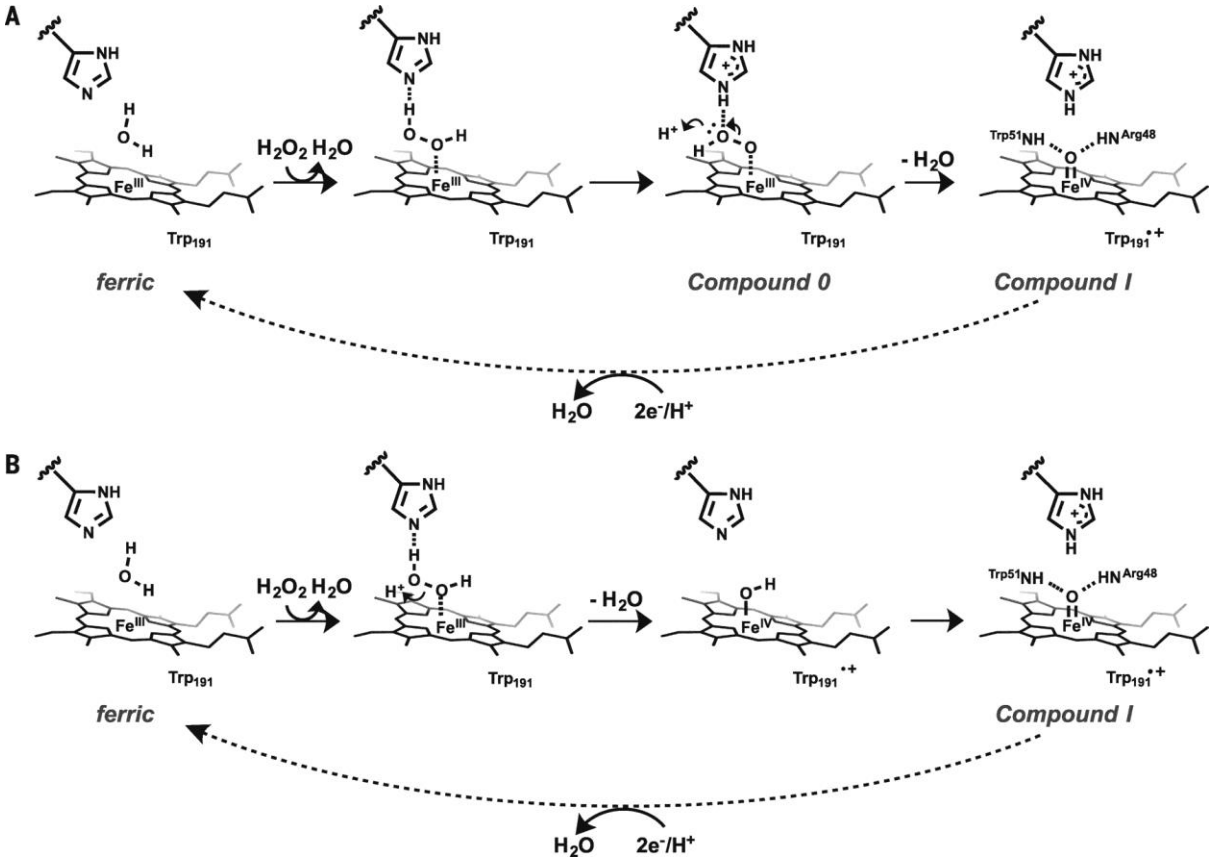

Fig. 3

Possible movement of protons during O–O bond activation.

(A) Formation of a peroxide-bound complex and then compound 0 is followed by O–O bond cleavage. The distal histidine retains a proton upon formation of compound I, which means that an additional proton is required for release of water in both formation and reduction of compound I. (See text for detailed discussion.) The orientation of deuterium atoms on active site water molecules

(Figs. 2 and 3) seems to preclude a water-mediated mechanism for O–O bond cleavage as suggested in horseradish peroxidase (34) because the deuterium atoms on W2 are oriented away from the ferryl oxygen atom and a hydrogen bond would not be possible (Fig. 2E). (B) An alternative mechanism from the same peroxide-bound complex. Cleavage of the peroxide bond may lead initially to formation of a transient iron(IV)-hydroxide species [Fe(IV)-OH], which, via proton transfer, leads to compound I, with Fe(IV)=O and a protonated distal histidine.

References and Notes

1. H. B. Dunford, Heme Peroxidases (Wiley, Chichester, UK, 1999).

2. P. R. Ortiz de Montellano, Cytochrome P450: Structure, Mechanism, and Biochemistry (Kluwer Academic/Plenum, New York, ed. 3, 2005).

3. K. D. Karlin, Bioinorganic chemistry: Model offers intermediate insight. Nature 463, 168–169 (2010).

4. S. G. Sligar, Glimpsing the critical intermediate in cytochrome P450 oxidations. Science 330, 924–925 (2010).

5. J. T. Groves, Enzymatic C-H bond activation: Using push to get pull. Nat. Chem. 6, 89–91 (2014).

6. I. Schlichting, J. Berendzen, K. Chu, A. M. Stock, S. A. Maves, D. E. Benson, R. M. Sweet, D. Ringe, G. A. Petsko, S. G. Sligar, The catalytic pathway of cytochrome P450cam at atomic resolution. Science 287, 1615–1622 (2000).

7. G. I. Berglund, G. H. Carlsson, A. T. Smith, H. Szöke, A. Henriksen, J. Hajdu, The catalytic pathway of horseradish peroxidase at high resolution. Nature 417, 463–468 (2002).

8. L. Que Jr., W. B. Tolman, Biologically inspired oxidation catalysis. Nature 455, 333–340 (2008).

9. A. R. McDonald, L. Que Jr., Iron-oxo complexes: Elusive iron(V) species identified. Nat. Chem. 3, 761–762 (2011).

10. J. Rittle, M. T. Green, Cytochrome P450 compound I: Capture, characterization, and C-H bond activation kinetics. Science 330, 933–937 (2010).

11. D. G. Kellner, S. C. Hung, K. E. Weiss, S. G. Sligar, Kinetic characterization of compound I formation in the thermostable cytochrome P450 CYP119. J. Biol. Chem. 277, 9641–9644 (2002).

12. R. K. Behan, M. T. Green, On the status of ferryl protonation. J. Inorg. Biochem. 100, 448–459 (2006). doi:10.1016/j.jinorgbio.2005.12.019 pmid:16500711Check here for full-text accesCrossRefPubMedWeb of ScienceGoogle Scholar

13. J. Terner, V. Palaniappan, A. Gold, R. Weiss, M. M. Fitzgerald, A. M. Sullivan, C. M. Hosten, Resonance Raman spectroscopy of oxoiron(IV) porphyrin pi-cation radical and oxoiron(IV) hemes in peroxidase intermediates. J. Inorg. Biochem. 100, 480–501 (2006). doi:10.1016/j.jinorgbio.2006.01.008 pmid:16513173Check here for full-text accesCrossRefPubMedWeb of ScienceGoogle Scholar

14. M. P. Blakeley, Neutron macromolecular crystallography. Crystallogr. Rev. 15, 157–218 (2009). doi:10.1080/08893110902965003Check here for full-text accesCrossRefGoogle Scholar

15. V. L. Davidson, Ion-protein coordination: The many faces of a proton. Nat. Chem. 3, 662–663 (2011). doi:10.1038/nchem.1122 pmid:21860447Check here for full-text accesCrossRefPubMedGoogle Scholar

16. M. P. Blakeley, A. J. Kalb, J. R. Helliwell, D. A. Myles, The 15-K neutron structure of saccharide-free concanavalin A. Proc. Natl. Acad. Sci. U.S.A. 101, 16405–16410 (2004). doi:10.1073/pnas.0405109101 pmid:15525703Check here for full-text accesAbstract/FREE Full TextGoogle Scholar

17. M. Sivaraja, D. B. Goodin, M. Smith, B. M. Hoffman, Identification by ENDOR of Trp191 as the free-radical site in cytochrome c peroxidase compound ES. Science 245, 738–740 (1989). doi:10.1126/science.2549632 pmid:2549632Check here for full-text accesAbstract/FREE Full TextGoogle Scholar

18. T. L. Poulos, S. T. Freer, R. A. Alden, S. L. Edwards, U. Skogland, K. Takio, B. Eriksson, N. Xuong, T. Yonetani, J. Kraut, The crystal structure of cytochrome c peroxidase. J. Biol. Chem. 255, 575–580 (1980). pmid:6243281Check here for full-text accesFREE Full TextGoogle Scholar

19. A. Gumiero, C. L. Metcalfe, A. R. Pearson, E. L. Raven, P. C. Moody, Nature of the ferryl heme in compounds I and II. J. Biol. Chem. 286, 1260–1268 (2011). doi:10.1074/jbc.M110.183483 pmid:21062738Check here for full-text accesAbstract/FREE Full TextGoogle Scholar

20. H. Hori, T. Yonetani, Powder and single-crystal electron paramagnetic resonance studies of yeast cytochrome c peroxidase and its peroxide and its peroxide compound, Compound ES. J. Biol. Chem. 260, 349–355 (1985). pmid:2981209Check here for full-text accesAbstract/FREE Full TextGoogle Scholar

21. S. L. Edwards, H. X. Nguyen, R. C. Hamlin, J. Kraut, Crystal structure of cytochrome c peroxidase compound I. Biochemistry 26, 1503–1511 (1987). doi:10.1021/bi00380a002 pmid:3036202Check here for full-text accesCrossRefPubMedGoogle Scholar

22. A. E. Pond, G. S. Bruce, A. M. English, M. Sono, J. H. Dawson, Spectroscopic study of the compound ES and the oxoferryl compound II states of cytochrome c peroxidase: Comparison with the compound II of horseradish peroxidase. Inorg. Chim. Acta 275–276, 250–255 (1998). doi:10.1016/S0020-1693(97)06106-9Check here for full-text accesCrossRefGoogle Scholar

23. J. E. Erman, T. Yonetani, A kinetic study of the endogenous reduction of the oxidized sites in the primary cytochrome c peroxidase-hydrogen peroxide compound. Biochim. Biophys. Acta 393, 350–357 (1975). doi:10.1016/0005-2795(75)90061-6 pmid:238609Check here for full-text accesCrossRefPubMedWeb of ScienceGoogle Scholar

24. J. E. Huyett, P. E. Doan, R. Gurbiel, A. L. P. Houseman, M. Sivaraja, D. B. Goodin, B. M. Hoffman, Compound ES of cytochrome-c peroxidase contains a Trp pi-cation radical: Characterization by continuous wave and pulsed Q-band external nuclear double resonance spectroscopy. J. Am. Chem. Soc. 117, 9033–9041 (1995). doi:10.1021/ja00140a021Check here for full-text accesCrossRefWeb of ScienceGoogle Scholar

25. Y. T. Meharenna, T. Doukov, H. Li, S. M. Soltis, T. L. Poulos, Crystallographic and single-crystal spectral analysis of the peroxidase ferryl intermediate. Biochemistry 49, 2984–2986 (2010). doi:10.1021/bi100238r pmid:20230048Check here for full-text accesCrossRefPubMedWeb of ScienceGoogle Scholar

26. A. J. Sitter, C. M. Reczek, J. Terner, Heme-linked ionization of horseradish peroxidase compound II monitored by the resonance Raman Fe(IV)=O stretching vibration. J. Biol. Chem. 260, 7515–7522 (1985). pmid:3997887Check here for full-text accesAbstract/FREE Full TextGoogle Scholar

27.H. B. Dunford, Peroxidases and Catalases: Biochemistry, Biophysics, Biotechnology, and Physiology (Wiley, Chichester, UK, ed. 2, 2010).Google Scholar

28. E. Derat, S. Shaik, The Poulos-Kraut mechanism of Compound I formation in horseradish peroxidase: A QM/MM study. J. Phys. Chem. B 110, 10526–10533 (2006). doi:10.1021/jp055412e pmid:16722763Check here for full-text accesCrossRefPubMedGoogle Scholar

29. S. Shaik, D. Kumar, S. P. de Visser, A. Altun, W. Thiel, Theoretical perspective on the structure and mechanism of cytochrome P450 enzymes. Chem. Rev. 105, 2279–2328 (2005).

doi:10.1021/cr030722j pmid:15941215Check here for full-text accesCrossRefPubMedWeb of ScienceGoogle Scholar

30. I. Efimov, S. K. Badyal, C. L. Metcalfe, I. Macdonald, A. Gumiero, E. L. Raven, P. C. Moody, Proton delivery to ferryl heme in a heme peroxidase: Enzymatic use of the Grotthuss mechanism. J. Am. Chem. Soc. 133, 15376–15383 (2011). doi:10.1021/ja2007017 pmid:21819069Check here for full-text accesCrossRefPubMedWeb of ScienceGoogle Scholar

31. T. L. Poulos, J. Kraut, The stereochemistry of peroxidase catalysis. J. Biol. Chem. 255, 8199–8205 (1980). pmid:6251047Check here for full-text accesFREE Full TextGoogle Scholar

32. T. H. Yosca, J. Rittle, C. M. Krest, E. L. Onderko, A. Silakov, J. C. Calixto, R. K. Behan, M. T. Green, Iron(IV)hydroxide pKa and the role of thiolate ligation in C–H bond activation by cytochrome P450. Science 342, 825–829 (2013). doi:10.1126/science.1244373 pmid:24233717Check here for full-text accesAbstract/FREE Full TextGoogle Scholar

33. J. E. Erman, L. B. Vitello, M. A. Miller, J. Kraut, Active-site mutations in cytochrome c peroxidase: A critical role for histidine-52 in the rate of formation of Compound I. J. Am. Chem. Soc. 114, 6592–6593 (1992). doi:10.1021/ja00042a068Check here for full-text accesCrossRefWeb of ScienceGoogle Scholar

34. P. Vidossich, G. Fiorin, M. Alfonso-Prieto, E. Derat, S. Shaik, C. Rovira, On the role of water in peroxidase catalysis: A theoretical investigation of HRP compound I formation. J. Phys. Chem. B 114, 5161–5169 (2010). doi:10.1021/jp911170bCheck here for full-text accesCrossRefPubMedGoogle Scholar

35. D. B. Goodin, M. G. Davidson, J. A. Roe, A. G. Mauk, M. Smith, Amino acid substitutions at tryptophan-51 of cytochrome c peroxidase: Effects on coordination, species preference for cytochrome c, and electron transfer. Biochemistry 30, 4953–4962 (1991). doi:10.1021/bi00234a017 pmid:1645185Check here for full-text accesCrossRefPubMedGoogle Scholar

36. C. Metcalfe, I. K. Macdonald, E. J. Murphy, K. A. Brown, E. L. Raven, P. C. Moody, The tuberculosis prodrug isoniazid bound to activating peroxidases. J. Biol. Chem. 283, 6193–6200 (2008). doi:10.1074/jbc.M707412200 pmid:18056997Check here for full-text accesAbstract/FREE Full TextGoogle Scholar

37. E. J. Murphy, C. L. Metcalfe, J. Basran, P. C. Moody, E. L. Raven, Engineering the substrate specificity and reactivity of a heme protein: Creation of an ascorbate binding site in cytochrome c

peroxidase. Biochemistry 47, 13933–13941 (2008). doi:10.1021/bi801480r pmid:19061385Check here for full-text accesCrossRefPubMedWeb of ScienceGoogle Scholar

38. M. P. Blakeley, S. C. Teixeira, I. Petit-Haertlein, I. Hazemann, A. Mitschler, M. Haertlein, E. Howard, A. D. Podjarny, Neutron macromolecular crystallography with LADI-III. Acta Crystallogr. D Biol. Crystallogr. 66, 1198–1205 (2010).

39. J. W. Campbell, LAUEGEN, an X-windows-based program for the processing of Laue diffraction data. J. Appl. Cryst. 28, 228–236 (1995).

40. J. W. Campbell, Q. Hao, M. M. Harding, N. D. Nguti, C. Wilkinson, LAUEGEN version 6.0 and INTLDM. J. Appl. Cryst. 31, 496–502 (1998).

41. S. Arzt, J. W. Campbell, M. M. Harding, Q. Hao, J. R. Helliwell, LSCALE - the new normalization, scaling and absorption correction program in the Daresbury Laue software suite. J. Appl. Cryst. 32, 554–562 (1999).

42. M. S. Weiss, Global indicators of x-ray data quality. J. Appl. Cryst. 34, 130–135 (2001).

43.Z. Otwinoski, W. Minor, Methods in Enzymology, vol. 276, Macromolecular Crystallography, Part A, C. W. Carter Jr., R. M. Sweet, Eds. (Academic Press, New York, 1997), pp. 307–326.Google Scholar

44. W. Kabsch, XDS. Acta Crystallogr. D Biol. Crystallogr. 66, 125–132 (2010). doi:10.1107/S0907444909047337 pmid:20124692Check here for full-text accesCrossRefPubMedWeb of ScienceGoogle Scholar

45. Collaborative Computational Project, Number 4, The CCP4 suite: Programs for protein crystallography. Acta Crystallogr. D Biol. Crystallogr. 50, 760–763 (1994).

46. P. D. Adams, P. V. Afonine, G. Bunkóczi, V. B. Chen, I. W. Davis, N. Echols, J. J. Headd, L. W. Hung, G. J. Kapral, R. W. Grosse-Kunstleve, A. J. McCoy, N. W. Moriarty, R. Oeffner, R. J. Read, D. C. Richardson, J. S. Richardson, T. C. Terwilliger, P. H. Zwart, PHENIX: A comprehensive Python-based system for macromolecular structure solution. Acta Crystallogr. D Biol. Crystallogr. 66, 213–221 (2010).

47. P. V. Afonine, M. Mustyakimov, R. W. Grosse-Kunstleve, N. W. Moriarty, P. Langan, P. D. Adams, Joint x-ray and neutron refinement with phenix.refine. Acta Crystallogr. D Biol. Crystallogr. 66, 1153–1163 (2010).

48. P. Emsley, K. Cowtan, Coot: Model-building tools for molecular graphics. Acta Crystallogr. D Biol. Crystallogr. 60, 2126–2132 (2004).

Acknowledgments: We thank D. Collison for assistance with EPR, P. Ortiz de Montellano for discussions on the mechanisms, S. Fisher for assistance with the joint x-ray/neutron refinement, and the University of Leicester BioMedical Workshop for custom building of microspectrophotometry equipment, and J Devos and the D-lab for experimental support. Atomic coordinates have been deposited in the Protein Data Bank under accession codes 4CVI for ferric CcP and 4CVJ for compound I. This work was supported by The Leverhulme Trust (grant F/00 212/Q to E.L.R./P.C.E.M.), Biotechnology and Biological Sciences Research Council (grant BB/C001184/1 to E.L.R./P.C.E.M., and a studentship to E.J.M.), The Wellcome Trust (grant WT094104MA to P.C.E.M./E.L.R.), an Institut Laue-Langevin studentship (to C.M.C.) and beam time at LADI-III and BIODIFF (EU FP7 NMI3-II grant 283883), Bruker UK (Sponsorship of A.J.F. and M.G.C.), and beam time at LADI-III and BIODIFF. P.C.E.M., M.P.B., and E.L.R. designed the research; C.M.C., A.G., M.P.B., A.O., S.C.M.T, T.E.S., C.L.M., E.J.M., and P.C.E.M. performed crystallographic experiments; C.M.C., A.G., M.P.B., S.C.M.T., A.O., T.E.S., E.L.R., and P.C.E.M. analyzed crystallographic data; C.M.C., A.J.F., M.G.C., J.B., and P.C.E.M. performed spectroscopic experiments; C.M.C, A.G., A.J.F, M.G.C., E.L.R., and P.C.E.M. analyzed spectra; and E.L.R., M.P.B., and P.C.E.M. wrote the paper, with contributions from all authors.